

# Murine photoplethysmography for *in vivo* estimation of vascular gold nanoshell concentration

## Gregory J. Michalak

Louisiana Tech University  
Department of Biomedical Engineering  
818 Nelson Avenue  
Ruston, Louisiana 71272

## Glenn P. Goodrich

## Jon A. Schwartz

Nanospectra Biosciences, Inc.  
8285 El Rio  
Suite 130  
Houston, Texas 77054

## William D. James

Texas A&M University  
Center for Chemical Characterization  
and Analysis  
College Station, Texas 77843

## D. Patrick O'Neal

Louisiana Tech University  
Department of Biomedical Engineering  
818 Nelson Avenue  
Ruston, Louisiana 71272

## 1 Introduction

Gold nanoshells have become a popular tool in biomedical optical imaging and tumor therapy because of their adjustable optical properties in the near-infrared region, their biocompatibility, and ability to passively extravasate in tumor targets.<sup>1</sup> In particular, these nanoparticles are highly optically dense because of their plasmon resonance and scattering cross section,<sup>2</sup> allowing them to be used in the laser-induced thermal ablation of optically accessible tumors at maximal penetration depths. In clinical practice, it is difficult to monitor the circulation of these nanoparticles after intravenous injection to predict delivery to the target tissue. Imaging techniques are useful to determine the biodistribution of these particles, and blood can be drawn and analyzed to determine the vascular concentration over time.<sup>3</sup> However, there is a need for a noninvasive system to determine the vascular concentration of these nanoparticles in real time to provide feedback during nanoparticle therapy.

Spectral analysis of blood components has been used in oximetry since the 1930's. Photo-oximetry exploits the spectral characteristics of deoxyhemoglobin and oxyhemoglobin to measure blood oxygen saturation (SpO<sub>2</sub>). The first devices measured the spectral change in extinction (and thus SpO<sub>2</sub>) when blood was removed via inflatable pressure induction and then reintroduced through normal perfusion into soft tissue.

**Abstract.** There is an urgent clinical need to monitor the intravenous delivery and bioavailability of circulating nanoparticles used in cancer therapy. This work presents the use of photoplethysmography for the noninvasive real-time estimation of vascular gold nanoshell concentration in a murine subject. We develop a pulse photometer capable of accurately measuring the photoplethysmogram in mice and determining the ratio of pulsatile changes in optical extinction between 805 and 940 nm, commonly referred to as  $R$ . These wavelengths are selected to correspond to the extinction properties of gold nanoshells. Six 30-s measurements (5 min, 2, 4, 6, 8, 10 h) are taken under light anesthesia to observe the change in  $R$  as the nanoparticles clear from the circulation. Our model describes the linear fit ( $R^2 = 0.85$ ) between  $R$  and the concentration of nanoparticles measured via *ex vivo* spectrophotometric and instrumental neutron activation analysis. This demonstrates the utility of this technique in support of clinical nanoparticle therapies. © 2010 Society of Photo-Optical Instrumentation Engineers. [DOI: 10.1117/1.3454374]

Keywords: gold nanoshells; pulse photometry; circulation half-life.

Paper 10207LR received Apr. 19, 2010; revised manuscript received May 19, 2010; accepted for publication May 21, 2010; published online Jul. 7, 2010.

An improvement in optical oximetry was made in the 1970's when the pulse oximeter was developed by the Nihon Kohden Corporation (Tokyo, Japan) employing two wavelengths to measure SpO<sub>2</sub>.<sup>4,5</sup> It measured a parameter, commonly referred to as  $R$ , which is an estimate of the ratio of the change in extinction at two wavelengths resulting from the pulsing arterial blood.

$$R = \frac{\log\left(\frac{V_{DC}}{V_{DC} - V_{AC}}\right)_{\lambda_1}}{\log\left(\frac{V_{DC}}{V_{DC} - V_{AC}}\right)_{\lambda_2}} \sim \frac{\left(\frac{V_{AC}}{V_{DC}}\right)_{\lambda_1}}{\left(\frac{V_{AC}}{V_{DC}}\right)_{\lambda_2}}$$

This parameter is estimated by using dc and ac portions of the photoplethysmogram (PPG), the waveform resulting from monitoring the intensity of light transmitted through pulsatile tissue and converting it into voltage using a photodetector circuit. Current pulse oximeters use this measured parameter and empirically derive a relationship between it and SpO<sub>2</sub>, since it is difficult to estimate the scattering characteristics of whole blood and tissue. Only recently have there been more advances in the algorithms used in pulse oximetry accounting for whole blood optical properties.<sup>6</sup>

Pulse oximetry was reported to be susceptible to interference from exogenous infrared extinguishing optical dyes injected into the body.<sup>7</sup> Many optical dyes are used during

Address all correspondence to: D. Patrick O'Neal, Louisiana Tech University, Department of Biomedical Engineering, 818 Nelson Ave, Ruston, LA, USA 71272. Tel: (318) 257-4420; Fax: (318) 257-4000; E-mail: dponeal@latech.edu

medical procedures such as hepatic studies,<sup>8</sup> renal studies, sentinel node detection in patients with cancer,<sup>9–11</sup> and cardiac output and volume measurements.<sup>12</sup> These dyes, including methylene blue, indigo carmine (IDG), indocyanine green (ICG), and patent blue, cause changes in the extinction spectrum of blood. Since many of these dyes show strong extinction in the NIR spectrum, their presence increases the optical density of blood at these wavelengths inducing a change in  $R$ , suggesting that the concentration of the dye could be quantified independently.

Pulse dye densitometry (PDD), a method based on pulse oximetry, is a noninvasive modality for measuring cardiac output and blood volume.<sup>13–15</sup> In PDD, an additional wavelength of light is used to match the extinction peak for a particular dye for comparison to an IR wavelength outside of the extinction spectrum of that dye. An accurate hemoglobin concentration, either assumed or invasively obtained, is used and  $R$  is measured. Upon injection of the dye,  $\Delta R$  is measured and used to calculate the arterial concentration of the dye. Recently developed PDD systems compatible with ICG<sup>16</sup> and IDG<sup>17</sup> employ at least one additional wavelength to account for tissue scattering by means of an algorithm incorporating the Beer-Lambert law for extinction and Schuster's theory of light scattering in dense media.

We present a novel instrument, a pulse photometer (PP), that measures murine PPG to quantify the vascular concentration of optically extinguishing nanoparticles. The purpose of our work was to build a noninvasive and inexpensive system capable of accurately measuring the PPG of a murine model and using it to monitor the concentration of circulating gold nanoshells having a circulation half-life of 3 to 6 h and a maximum accumulation at 24 h.<sup>18</sup>

Historically, it is a technique that has proven problematic in murine models because of the difficulty in obtaining a strong pulsatile signal from a small extremity such as the foot or tail of a mouse. This problem would be mitigated in a device for human use because of the higher magnitude of the pulsatile signal. However, murine testing is an integral part of nanoshell quality control, which further emphasizes the need for a murine compatible optical tracking system. This work presents an initial study of monitoring the change in  $R$  with changing nanoshell concentration using our device. We show that it can measure a stable PPG and be removed and reattached at later time points, making it compatible with long circulating nanoparticle therapy.

## 2 Materials and Methods

### 2.1 Nanoshells

Gold-coated silica-core nanoshells conjugated with a monolayer of poly(ethylene glycol), reported to be 160 to 170 nm in diameter, were obtained from Nanospectra Biosciences, Incorporated (Houston, Texas). We measured the extinction of the delivered batch in a UV/VIS spectrophotometer [Beckman Coulter (Brea, California) DU 800]. The optical densities of the batch were 119.82 and 95.53  $\text{cm}^{-1}$  at 805 and 940 nm, respectively.

### 2.2 Blood Collection and External Analysis

All animals were handled and cared for in accordance with the Louisiana Tech Institutional Animal Care and Use Com-

mittee. Five female BALB/c "retired breeder" mice (Harlan, Indianapolis, Indiana), weighing between 26 and 32 g, were used in this study. Concurrent to measurements taken with our device, blood was sampled from each subject at each time point and analyzed with our spectrophotometer in a similar manner to that previously reported.<sup>19</sup> A 5- $\mu\text{L}$  blood draw was taken from the tail and diluted into a microcuvette [Brandtech (Essex, Connecticut) Ultra-Micro] containing 95  $\mu\text{L}$  of 10% Triton X-100 to eliminate scattering blood cells from the sample. The extinction at 805 was then measured. Then, an additional 100  $\mu\text{L}$  of Triton X was added to the sample to resolve the strong extinction of oxyhemoglobin at 560 nm. The sample was scanned again, and the extinction at 560 nm was used to establish the hemoglobin concentration using a standard oxyhemoglobin spectrum. This value was used to subtract the contribution of oxyhemoglobin from the extinction at 805 nm in the original sample, and calculate the extinction caused by the nanoshells. This value was then scaled by the dilution factor to calculate the optical density of the nanoshells in the whole blood.

Our *ex vivo* spectrophotometric technique was validated by comparison to instrumental neutron activation analysis (INAA). After analysis with spectrophotometry, the blood samples were then transferred to INAA vials, dried, and delivered to the Texas A&M Elemental Analysis Laboratory for analysis similar to what has been previously reported.<sup>18</sup> The gold content (micrograms) in each vial was determined and compared to the measurements taken using spectrophotometry.

### 2.3 Instrumentation

Our device consists of a probe compatible with mouse anatomy, analog circuitry, a data acquisition card, and LabVIEW software. The probe is a clip that fits gently on the foot of the animal. It contains a multiwavelength LED that emits light at four wavelengths [Marubeni (Santa Clara, California) L660/735/805/940-40B42], two of which are used in our measurements (805 and 940 nm), and a photodiode (Hamamatsu S1337-33BR) that collects the emitted light through the foot. The analog circuitry consists of a timing module to control the synchronous firing and collection of each wavelength, a current to voltage converter to amplify the signals from the photodiode, and filters to precondition the signals before digitization. A schematic of this circuitry can be seen in Fig. 1.

The data acquisition card collects the data from the circuitry and imports it into LabVIEW in one second waveforms on separate channels for analysis. A separate channel collects data while no wavelengths are emitted, and is used to subtract the signals due to ambient light from the signals while the LEDs are emitting. The LabVIEW software then separates each channel into its ac and dc portions. A bandpass filter (4- to 10-Hz passband corresponding to heart rates between 240 and 600 bpm) is applied to the ac signals to remove unwanted frequencies. The parameter  $R$  is then computed in real time, using the right half of the previous equation, where  $\lambda_1=805$  nm and  $\lambda_2=940$  nm.

### 2.4 Data Collection

Prior to injection of nanoshells, the animal was anesthetized with isoflurane vaporized (Dentry Biomedical, Incorporated,

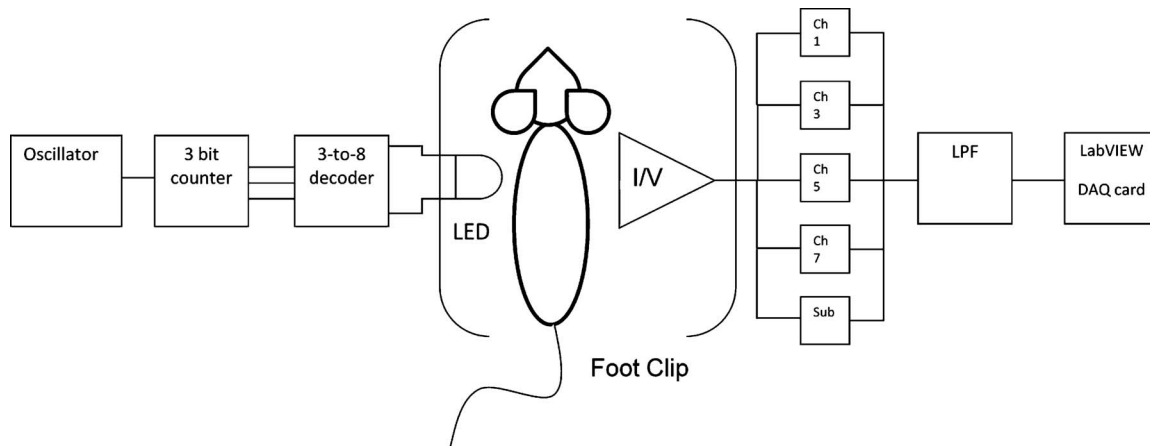


**Fig. 1** Schematic diagram of the circuitry used to collect the PPG from the mouse's foot.

Hunt Valley, Maryland, Isoflurane Vaporizer) with 95% oxygen delivered with an oxygen concentrator (Invacare 5, Elyria, Ohio) and the tail vein was catheterized with a 29 gauge needle connected to polyurethane tubing. The concentrator delivered anesthesia as well as maintained stable blood oxygen saturation during the measurement. Once the vein was catheterized, the animal was placed on a feedback controlled heating pad [Physitemp (Clifton, New Jersey) TCAT-2LV Controller] set to 40 °C to stabilize the core temperature and induce vasodilation. Vasodilation enhanced the peripheral circulation and thus the detected ac signal strength. Once temperature stabilization was achieved, the probe was placed on the animal's foot and the PP was allowed to collect data. 30-s averages of the values of  $R$  were computed to assess signal stability. Anticipating potential transient problems such as motion artifact or low perfusion, the signal was deemed acceptable once the ac magnitude was above 5 mV peak-to-peak and the standard deviation of  $R$  was less than 0.03. This  $R$ , assessed at near blood oxygen saturation, was used as a baseline for all subsequent measurements in that subject. A bolus injection of nanoshells at 4.5  $\mu\text{L}/\text{g}$  was then given via the tail vein and  $\Delta R$  was measured. To find the  $\Delta R$  for each time point, the baseline reading from that particular animal was subtracted from the current  $R$  measurement. An example of instantaneous  $R$  measurements after injection can be seen in Fig. 2.

Nanoshells are more optically dense at 805 nm compared to 940 nm, and thus  $R$  will be seen to increase on injection and decrease to the baseline as the particles are cleared from circulation. After approximately 5 min of data collection, the last 30-s average meeting the previously stated criteria was used as  $R$  for the first time point. The probe was then removed and a 5- $\mu\text{L}$  blood draw was then taken, analyzed with our spectrophotometer, and stored for later INAA analysis. Subsequent  $\Delta R$  measurements via probe reattachment and *ex vivo* blood analysis were taken from each animal at 2, 4, 6, 8, and 10-h postinjection.

### 3 Results

We examined the baseline measurements of  $R$  from each subject taken before injection of nanoshells, and found little de-

viation from the average ( $0.7962 \pm 0.0102$  SD). This indicated that blood oxygenation was stable for each animal under anesthesia, and that minor changes in probe coupling to the animal's foot did not significantly influence the measurement of  $R$ . At all points after injection,  $\Delta R$  with respect to baseline was calculated.  $\Delta R$ , concomitant with the *ex vivo* analysis of blood draws analyzed with UV/VIS spectrophotometry, showed a gradual decrease toward 0 in subsequent measurements as the nanoshells were cleared from the vasculature (Fig. 3).

A linear model of the optical density via UV/VIS of the nanoshells in whole blood with respect to  $\Delta R$  was produced from measurements taken from all five animals (Fig. 4).  $R$  statistical software was used for all data analysis. The data showed a linear fit with a nonsignificant  $y$  intercept ( $y = 24.54x - 0.0085$ ,  $R^2 = 0.85$ ,  $p = 2.875 \times 10^{-13}$ ). Confidence and prediction intervals ( $\alpha = 0.05$ ) were produced for the model. The data lie within the prediction interval for all measured values of  $\Delta R$ , indicating that the model could predict future values of the nanoshell optical density with 95% confidence. Influence diagnostics [difference in betas (DFBE-

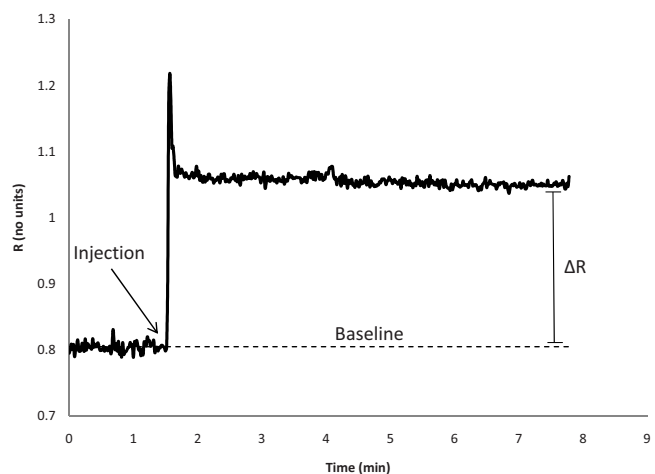


**Fig. 2**  $\Delta R$  measured after the injection of nanoshells. A plot of the instantaneous value of  $R$  shows a relatively constant baseline measurement and an increase after injection.

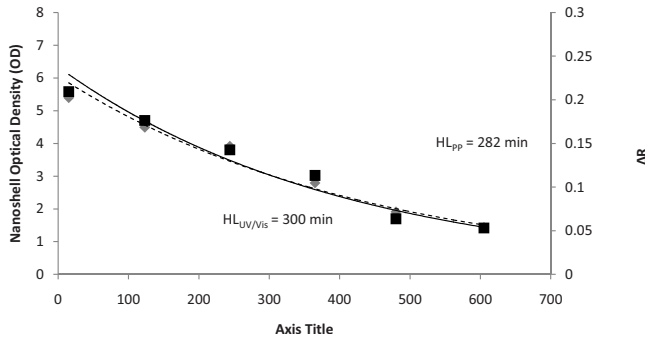


**Fig. 3** Dual-axis plot of  $\Delta R$  (black squares) and nanoshell optical density (gray diamonds) over time from one mouse.

TAS), Cook’s distance, and hat matrix examination] and residual analysis did not suggest the presence of influential data points or outliers. The average half-lives of nanoshell circulation using a single exponential fit [ $hl = -(\ln 0.5) \cdot \tau$ ] of the five subjects measured with the PP and with UV/VIS were  $320.8 \pm 86.6$  min and  $318.6 \pm 81.4$  min, respectively. The circulation half-lives and the average heart rate measured with the PP for each animal can be seen in Table 1.

A linear model comparing UV/VIS to INAA measurements showed excellent correlation ( $y = 0.0434x - 0.1948$ ,  $R^2 = 0.98$ ,  $p = 2.2 \times 10^{-16}$ ), confirming the ability of the spectrophotometric technique to accurately measure nanoshell optical density (Fig. 5). The low-volume cuvettes (100  $\mu\text{L}$ ) used in conjunction with a UV/VIS spectrophotometer employing a focused microbeam design made this possible. The INAA data (micrograms) compared to  $\Delta R$  showed a high correlation similar to the comparison of UV/VIS with  $\Delta R$  ( $y = 4.795x - 0.0396$ ,  $R^2 = 0.85$ ,  $p = 6.38 \times 10^{-13}$ ).

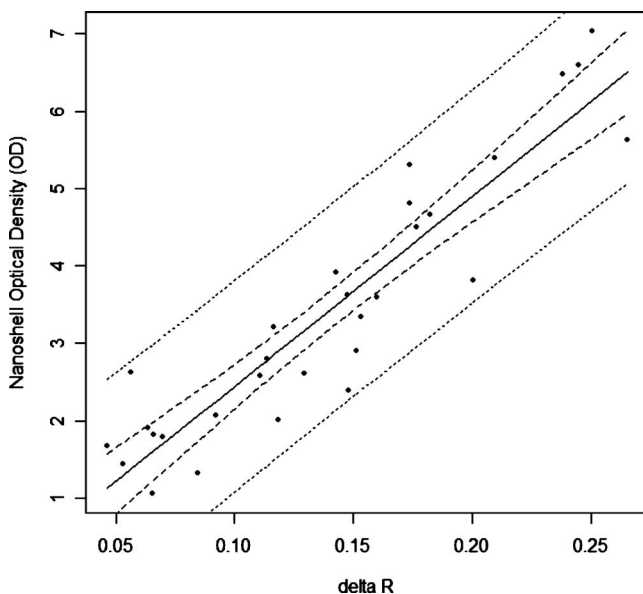


**Fig. 4** Linear plot of nanoshell optical density by UV/VIS spectrophotometry with respect to  $\Delta R$  measured with the pulse photometer with 95% confidence (dashed line) and prediction (dotted line) intervals shown ( $n = 30$ ).

**Table 1** Circulation half-lives measured using pulse photometry and UV/VIS spectrophotometry with the corresponding average heart rate of each subject.

Mouse	$HL_{pp}$ (min)	$HL_{UV/VIS}$ (min)	Average HR (bpm)
1	454	273	$415 \pm 26$
2	296	232	$408 \pm 27$
3	348	445	$384 \pm 56$
4	282	300	$368 \pm 23$
5	224	343	$391 \pm 14$

#### 4 Conclusions

We demonstrate the use of photoplethysmography for monitoring vascular nanoshell concentration in murine models. It is evident that nanoshell concentration is directly related to  $\Delta R$ , suggesting that the pulse photometer can be calibrated to directly estimate the vascular concentration of nanoshells in future experiments. Analysis of the data reveals that our device is capable of accurately measuring  $\Delta R$  both immediately after injection of nanoshells and in subsequent measurements taken after probe reattachment. The lack of evidence of outliers or overly influential data points indicates that erroneous measurements of  $R$  made by our PP are rare under controlled conditions. Figure 4 demonstrates deviations from the linear model used to determine the nanoshell optical density from  $\Delta R$ . This is most likely due to small wavelength-dependant changes in optical path length and probing volume when coupling the probe to the foot of the mouse. Since we are attempting to measure values of  $\Delta R$  in the interval of 0 to 0.3,

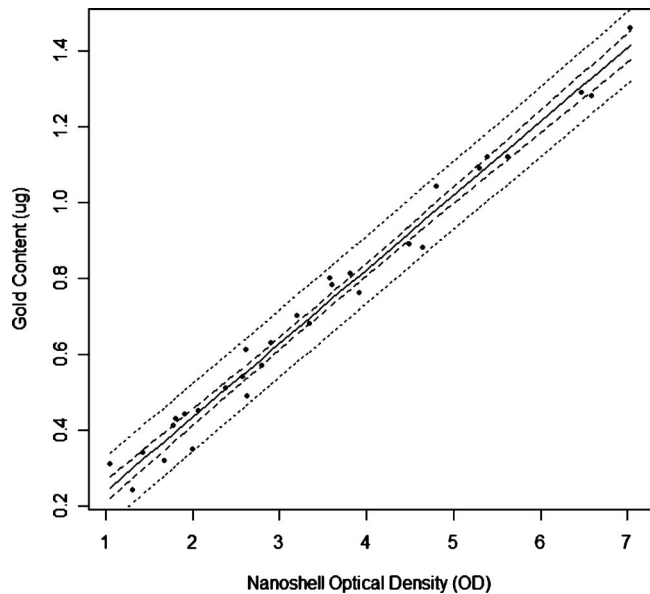


**Fig. 5** Linear model validating the measurements of nanoshell optical density, measured with UV/VIS spectrophotometry, by comparison to gold content measured by INAA. The 95% confidence (dashed line) and prediction (dotted line) intervals are shown.

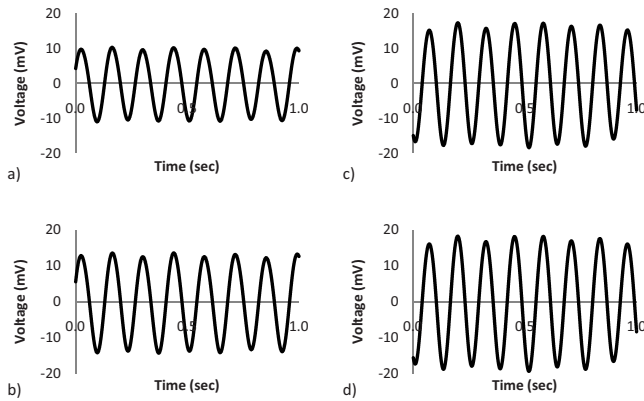


**Fig. 6** Pulsatile waveforms before injection of nanoshells at (a) 805 nm, (b) 940 nm, and after injection (c) 805 nm, and (d) 940 nm.

small changes in probe coupling would affect the measurements. Noise that was inherent to the instrument did not appear to have a significant effect on the PPG signal, as evident by the signal strength and stability of the filtered pulsatile waveforms at both wavelengths before and after injection of nanoshells, shown in Fig. 6.

Thus far, we have developed a linear empirical model that is accurate, given that blood oxygenation is maintained. We plan to improve this device by adapting the principles of PDD and pulse oximetry to calculate the vascular nanoshell concentration by incorporating the contribution of blood attenuation coefficients to the pulsatile change in extinction of light.

#### Acknowledgments

The authors wish to acknowledge the Office of the Vice President for Research and the Nuclear Science Center at Texas A&M University, respectively, for support for the reactor irradiations made in connection with the NAA measurements, and for providing those irradiations. We also wish to thank Elyse Orchard from Louisiana State University Health Science Center at Shreveport for instruction and the loan of anesthesia delivery equipment. This work was funded by a grant from the Louisiana Board of Regents Industrial Ties Research Subprogram [LEQSF(2009-12)-RD-B-07].

#### References

1. D. P. O'Neal, L. R. Hirsch, N. J. Halas, J. D. Payne, and J. L. West, "Photo-thermal tumor ablation in mice using near infrared-absorbing nanoparticles," *Cancer Lett.* **209**, 171–176 (2004).
2. S. J. Oldenburg, R. D. Averitt, S. L. Westcott, and N. J. Halas, "Nanoengineering of optical resonances," *Chem. Phys. Lett.* **28**, 243–247

- (1998).
3. D. P. O'Neal, L. R. Hirsch, N. J. Halas, J. D. Payne, and J. L. West, "Photo-thermal cancer therapy using intravenously injected near infrared-absorbing nanoparticles," *Proc. SPIE* **5689**, 149–157 (2005).
4. W. J. Severinghaus and Y. Honda, "History of blood gas analysis. VII. Pulse oximetry," *J. Clin. Monit.* **3**, 135–138 (1987).
5. T. Aoyagi and K. Miyasaka, "Theory and applications of pulse spectrophotometry," *Anesth. Analges.* **94**(1 Suppl.), S93–S95 (2002).
6. T. Aoyagi, M. Fuse, N. Kobayashi, K. Machida, and K. Miyasaka, "Multiwavelength pulse oximetry: theory for the future," *Anesthes. Analges.* **105**, S53–S58 (2007).
7. M. S. Scheller, R. J. Unger, and M. J. Kelner, "Effects of intravenously administered dyes on pulse oximetry readings," *Anesthesiology* **65**, 550–552 (1986).
8. S. G. Sakka, K. Reinhart, and A. Meier-Hellmann, "Comparison of invasive and noninvasive measurements of indocyanine green plasma disappearance rate in critically ill patients with mechanical ventilation and stable hemodynamics," *Intensive Care Med.* **26**, 1553–1556 (2000).
9. L. Heuter, K. Schwartzkopf, and W. Karzai, "Interference of patent blue V dye with pulse oximetry and co-oximetry," *Eur. J. Anaesthesiol.* **22**, 471–484 (2005).
10. L. Vokach-Brodsky, S. S. Jeffery, H. J. M. Lemmens, and J. G. Brock-Utne, "Isosulfane blue affects pulse oximetry," *Anesthesiology* **93**, 1002–1003 (2000).
11. R. W. Hoskin and R. Granger, "Intraoperative decrease in pulse oximeter readings following injection of isosulfan blue," *Can. J. Anaesth.* **3**, 38–40 (2000).
12. T. Imai, C. Mitaka, T. Nosaka, A. Koike, S. Ohki, Y. Isa, and F. Kunitomo, "Accuracy and repeatability of blood volume measurement by pulse dye densitometry compared to the conventional method using  $^{51}\text{Cr}$ -labeled red blood cells," *Intensive Care Med.* **26**, 1343–1349 (2000).
13. T. Iijima, T. Aoyagi, Y. Iwao, J. Masuda, M. Fuse, N. Kobayashi, and H. Sankawa, "Cardiac output and circulating blood volume analysis by pulse dye-densitometry," *J. Clin. Monit.* **31**, 81–89 (1997).
14. W. Baulig, O. Bernhard, D. Bettex, D. Schmidlin, and E. R. Schmid, "Cardiac output measurement by pulse dye densitometry in cardiac surgery," *Anaesthesia* **60**, 968–973 (2005).
15. M. Haruna, K. Kumon, N. Yahagi, Y. Watanabe, Y. Ishida, N. Kobayashi, and T. Aoyagi, "Blood volume measurement at the bedside using ICG pulse spectrophotometry," *Anesthesiology* **89**, 1322–1328 (1998).
16. N. Taguchi, S. Nakagawa, K. Miyasaka, M. Fuse, and T. Aoyagi, "Cardiac output measurement by pulse dye densitometry using three wavelengths," *Pediatr. Crit. Care Med.* **5**(4), 343–350 (2004), <http://www.ncbi.nlm.nih.gov/pubmed/15215003>.
17. Y. Fujita, T. Yamamoto, M. Fuse, N. Kobayashi, S. Takeda, and T. Aoyagi, "Pulse dye densitometry using indigo carmine is useful for cardiac output measurement, but not for circulating blood volume measurement," *Eur. J. Anaesthesiol.* **21**, 632–637 (2004).
18. W. D. James, L. R. Hirsch, J. L. West, P. D. O'Neal, and J. D. Payne, "Application of INAA to the build-up and clearance of gold nanoshells in clinical studies in mice," *J. Radioanal. Nucl. Chem.* **271**(2), 455–459 (2007).
19. G. J. Michalak, H. A. Anderson, and D. P. O'Neal, "Feasibility of using a two-wavelength photometer to estimate the concentration of circulating near-infrared extinguishing nanoparticles," *J. Biomed. Nanotechnol.* **6**(1), 73–81 (2010).